

# Heat Transfer Characteristics of a Masonry Cavity Wall

**REFERENCE:** Van Geem, M. G., "Heat Transfer Characteristics of a Masonry Cavity Wall," *Thermal Insulation: Materials and Systems, ASTM STP 922*, F. J. Powell and S. L. Matthews, Eds., American Society for Testing and Materials, Philadelphia, 1987, pp. 318-342.

**ABSTRACT:** Heat transfer characteristics of building elements must be known to evaluate energy losses through a building envelope. Laboratory tests of walls under dynamic temperature conditions provide data that can be used to determine thermal properties. Dynamic testing is particularly important for massive envelope components that store as well as transmit heat.

A block-brick cavity wall was tested in the calibrated hot box facility at the Construction Technology Laboratories, a division of the Portland Cement Association. The wall consisted of 100-mm (4-in.) clay brick on the exterior face, a 70-mm (2<sup>3</sup>/<sub>4</sub>-in.) cavity, 150-mm (6-in.) concrete block, and 3 mm (1/8 in.) of plaster on the interior face. Metal rectangular ties were used for tying brick and block wythes.

Laboratory tests were performed on the wall with and without expanded perlite fill in the cavity. The wall was subjected to steady-state, transient, and periodically varying temperature conditions. Steady-state results are used to define heat transmission coefficients, such as  $U$  and  $R$  values. Data obtained during transient and periodic temperature variations are used to define dynamic thermal response of the wall. Dynamic response includes heat storage capacity as well as heat transmission characteristics of the wall assembly. Test data are also used to determine the effects of perlite insulation in the cavity.

The cavity wall construction is similar to that of a test building monitored by the National Bureau of Standards (NBS) in Gaithersburg, Maryland. Two of the dynamic temperature cycles applied to the wall during laboratory tests were derived from actual wall surface temperatures at the NBS test building. Heat flow meter data from the test building are compared with calibrated hot box test results.

Laboratory test results provide a data base for evaluation of building envelope performance where cavity walls are used. The results also provide information on the effectiveness of expanded perlite as a cavity-fill material.

**KEY WORDS:** buildings, calibrated hot box, cavity walls, concrete, energy, heat transmission, masonry, thermal resistance, thermal inertia, thermal insulation

## Nomenclature

- $q_{ss}$  = Heat flux predicted from steady-state analysis
- $q_w$  = Heat flux measured by calibrated hot box
- $t_i$  = Indoor chamber air temperature
- $t_1$  = Wall surface temperature, indoor side
- $t_3$  = Block temperature on surface facing cavity
- $t_4$  = Brick temperature on surface facing cavity
- $t_2$  = Wall surface temperature, outdoor side
- $t_o$  = Outdoor chamber air temperature

<sup>1</sup>Senior research engineer, Construction Technology Laboratories, Portland Cement Association, Skokie, IL 60077.

Tests were conducted to evaluate thermal performance of a masonry cavity wall with and without expanded perlite loose-fill insulation. Steady-state test results were used to obtain average heat transmission coefficients including total thermal resistance,  $R_T$ , and thermal transmittance,  $U$ . Data obtained during periodic temperature variations were used to define dynamic thermal response under selected temperature ranges.

The wall with expanded perlite insulation is similar to walls of a test building monitored by the National Bureau of Standards (NBS) in Gaithersburg, Maryland. Two of the dynamic temperature cycles applied to the wall during laboratory tests were derived from actual wall surface temperatures of the NBS test building.

A third temperature cycle, a simulated sol-air cycle, was selected to permit comparison of results with walls previously tested [1-6].

The objectives of the experimental investigation were to evaluate and compare the performance of walls with and without expanded perlite insulation and to compare laboratory results with NBS field test results. The walls were tested in the calibrated hot box facility of the Portland Cement Association's Construction Technology Laboratories (CTL).

### Test Specimens

A 300-mm (12-in.) block-brick cavity wall without insulation and the same wall with expanded perlite loose-fill insulation were tested in the calibrated hot box. The walls were built using techniques representative of field construction practices. The overall nominal wall dimensions were 2.62 by 2.62 m (103 by 103 in.).

### Wall Construction

The 300-mm (12-in.) uninsulated, reinforced block-brick cavity wall, designated Wall M9, was constructed of 143-mm (5<sup>5</sup>/<sub>8</sub>-in.) concrete block and 86-mm (3<sup>3</sup>/<sub>8</sub>-in.) clay brick separated by a 70-mm (2<sup>3</sup>/<sub>4</sub>-in.) air space. The measured unit weight of the wall was 395 kg/m<sup>2</sup> (81 lb/ft<sup>2</sup>). The average measured wall thickness was 305 mm (12 in.). The measured wall area perpendicular to heat flow was 6.84 m<sup>2</sup> (73.7 ft<sup>2</sup>).

Two-core concrete block was used to construct the wall. Measured unit weights of the oven-dry block and brick were 1980 kg/m<sup>3</sup> (124 lb/ft<sup>3</sup>) and 2160 kg/m<sup>3</sup> (135 lb/ft<sup>3</sup>), respectively. The measured solid volume percentages of the block and brick were 56 and 82%, respectively. The measured moisture contents of the block and brick after the calibrated hot box tests had been completed were 1.2 and 0.3% of the oven-dry weight, respectively.

The mortar consisted of one part Type S masonry cement to three parts masonry sand by volume. The block and brick were laid in a running bond pattern. The joints were tooled. Metal rectangular ties were placed across the cavity at every other block joint. The tie dimensions are given in Ref 7.

A 3-mm (1/8-in.)-thick smooth plaster coating was applied to the inside block surface. The plaster consisted of one part Type S masonry cement to 2<sup>1</sup>/<sub>2</sub> parts masonry sand by volume. Two coats of off-white flat latex paint were applied to the plaster prior to testing.

### Instrumentation

Thermocouples corresponding to the ASTM Temperature Electromotive Force (EMF) Tables for Standardized Thermocouples (E 230-83), Type T, were used to measure temperatures. The thermocouples were located on the indoor and outdoor wall faces, on the interior faces of the cavity, and in the air space of each chamber.

Sixteen thermocouples were taped to the indoor plaster surface. On the outdoor wall face,

eight thermocouples were taped to vertical mortar joints, and eight were taped to brick. The thermocouples were uniformly distributed on a 500-mm (20-in.)-square grid over the wall area.

Thermocouples taped to the cavity side of the block face were also uniformly distributed on a 500-mm (20-in.)-square grid. The 16 thermocouples were wired so that electrical averages of four thermocouple junctions, located along a horizontal line across the grid, were obtained.

Thermocouples on the cavity side of the brick face were embedded in the horizontal mortar joints closest to the grid pattern of the other thermocouples. The thermocouple junctions were located 6 to 13 mm ( $1/4$  to  $1/2$  in.) into the back of the plane of the brick surface facing the cavity. The thermocouples on this surface were also wired to obtain one average reading of four thermocouples in a horizontal row. Average temperatures reported for this surface were an average reading of twelve thermocouples because one row of thermocouples gave erroneous readings.

Surface thermocouples were securely attached to the wall over a length of approximately 75 mm (3 in.). The tape covering the sensors on the indoor side was painted the same color as the plaster surface. Gray tape used on other surfaces was not painted.

Sixteen thermocouples were used to measure temperatures in the air space of each chamber. The thermocouples were uniformly distributed on the same 500-mm (20-in.) grid over the wall area as the other thermocouples and were located approximately 75 mm (3 in.) from the face of the test wall.

#### *Addition of Expanded Perlite Insulation*

After Wall M9 was tested, the cavity was filled with expanded perlite loose-fill insulation. The wall was redesignated Wall M10 and tested in the calibrated hot box. Figures 1 and 2 show the outside and inside surfaces of Wall M10 after tests were completed.

The silicone-treated expanded perlite, as received, had a unit weight of  $69 \text{ kg/m}^3$  ( $4.3 \text{ lb/ft}^3$ ). The measured unit weight of Wall M10 was  $400 \text{ kg/m}^2$  ( $82 \text{ lb/ft}^2$ ).

The top portion of the test frame was removed after calibrated hot box tests were completed to determine whether the expanded perlite insulation had settled. At the end of the calibrated hot box tests, 3% of the cavity area perpendicular to heat flow did not contain expanded perlite insulation. Locations of expanded perlite voids are illustrated in Fig. 3.

Insulation settlement was probably accelerated by vibrations from dynamic load testing at a site located approximately 9 to 18 m (30 to 60 ft) from the calibrated hot box. Dynamic load tests occurred most of the time the cavity wall was being tested.

#### **NBS Test Building No. 6**

The National Bureau of Standards (NBS) constructed six one-room test buildings in Gaithersburg, Maryland, to determine the effect of wall mass on heating and cooling loads of residential buildings. The 6.1 by 6.1-m (20 by 20-ft) buildings have the same floor plan and orientation. The buildings are identical except for materials used for wall construction. The six buildings were extensively instrumented for measuring heating loads, cooling loads, wall heat transmission, indoor temperature, and humidity [8].

Test Building 6 has walls similar to the insulated cavity wall tested in the calibrated hot box. The walls were constructed of hollow core concrete block and clay brick separated by a 89-mm ( $3\frac{1}{2}$ -in.) cavity containing expanded perlite loose-fill insulation. The nominal dimensions of the block and brick were 200 mm (8 in.) and 100 mm (4 in.), respectively. The block weighed  $1680 \text{ kg/m}^3$  ( $105 \text{ lb/ft}^3$ ) [8].

#### **Calibrated Hot Box Test Facility**

The block-brick cavity wall with and without expanded perlite loose-fill insulation was tested in the calibrated hot box facility shown in Figs. 4 and 5. Tests were performed in accordance

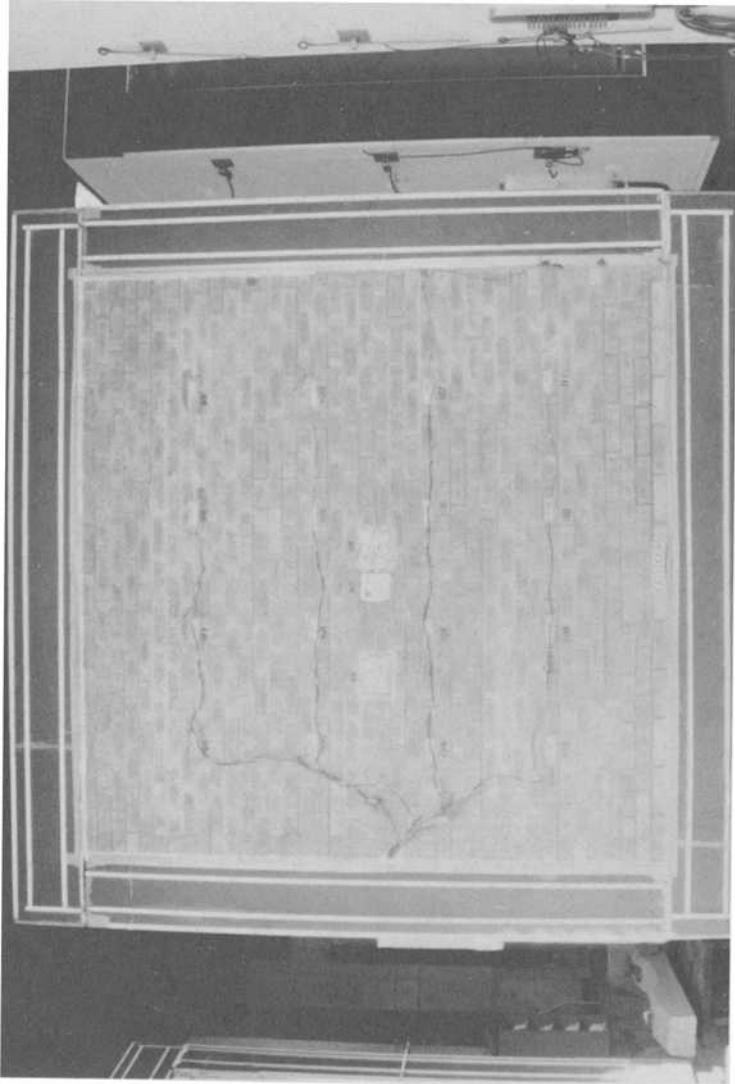


**FIG. 1**—*Wall M10 outdoor surface after testing.*

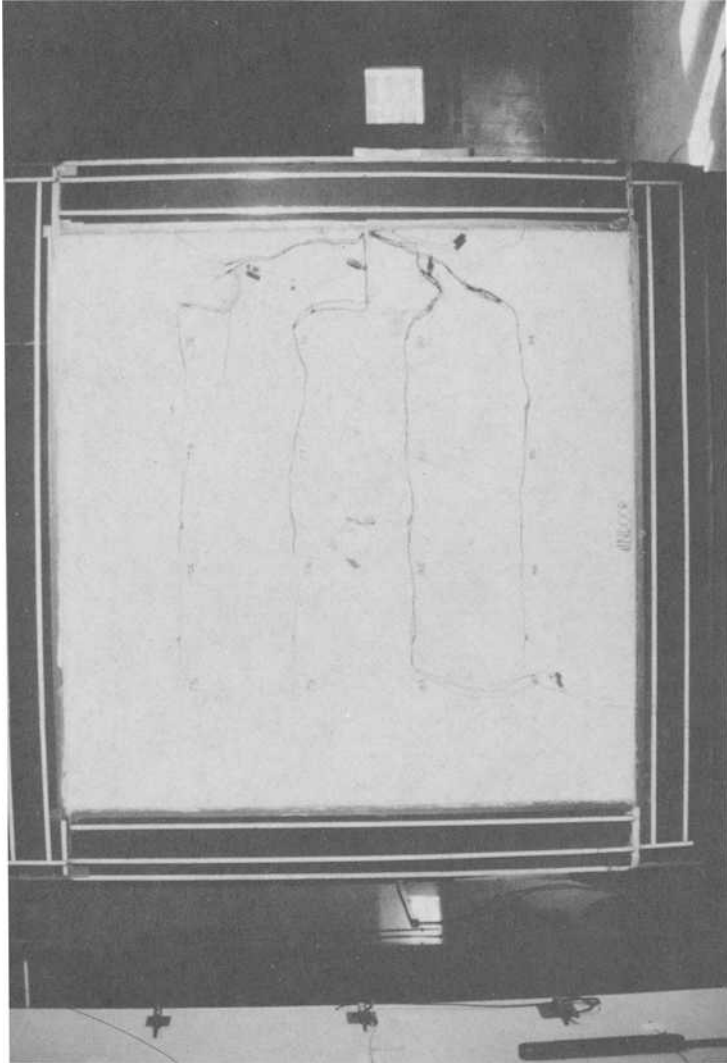


**FIG. 2—Wall M10 indoor surface after testing.**

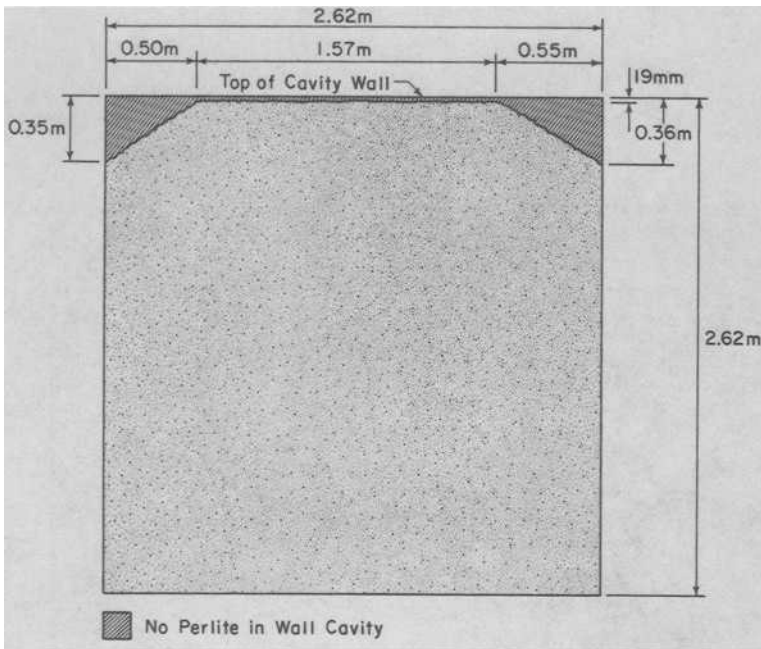


FIG. 3—Locations of expanded perlite voids after the calibrated hot box tests.

with the ASTM Test for Thermal Performance of Building Assemblies by Means of a Calibrated Hot Box (C 976-82).

The following is a brief description of the calibrated hot box. Instrumentation and calibration details are described in Refs 7 and 9. The facility consists of two highly insulated chambers, as shown in Fig. 5. The walls, ceiling, and floors of each chamber are insulated with foamed urethane sheets to obtain a nominal thickness of 300 mm (12 in.). During tests, the chambers are clamped tightly against an insulated frame that surrounds the test wall. Air in each chamber is conditioned by heating and cooling equipment to obtain desired temperatures on each side of the test wall.

The outdoor (climatic) chamber can be held at a constant temperature or cycled between  $-26$  and  $54^{\circ}\text{C}$  ( $-15$  and  $130^{\circ}\text{F}$ ). Temperature cycles can be programmed to obtain the desired time-temperature relationship. The indoor (metering) chamber, which simulates an indoor environment, can be maintained at a constant room temperature between  $18$  and  $27^{\circ}\text{C}$  ( $65$  and  $80^{\circ}\text{F}$ ).

The facility was designed to accommodate walls with thermal resistance values ranging from  $0.26$  to  $3.52 \text{ m}^2 \cdot \text{K}/\text{W}$  ( $1.5$  to  $20 \text{ h} \cdot \text{ft}^2 \cdot ^{\circ}\text{F}/\text{Btu}$ ).

Heat flow through a test specimen is determined from measurements of the amount of energy input to the indoor chamber to maintain a constant temperature. The measured energy input must be adjusted for heat losses. Since the net energy into the indoor chamber equals zero, heat transfer through the test wall can be expressed by the following energy balance equation.

$$Q_w = Q_c - Q_h - Q_{fan} - Q_l - Q_f \quad (1)$$

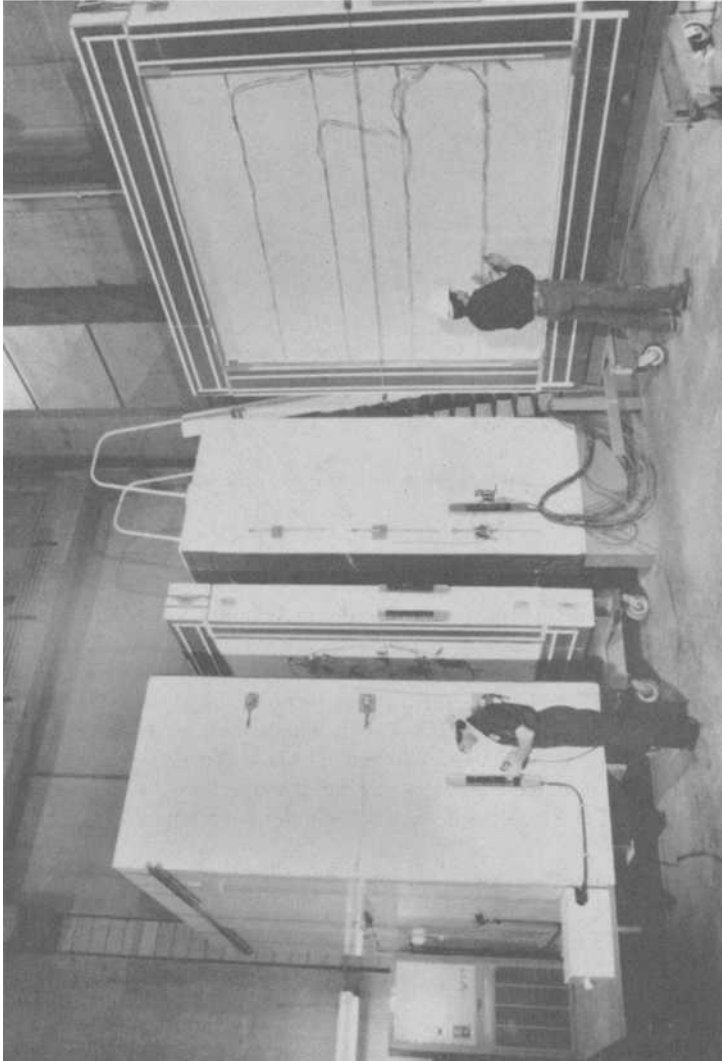


FIG. 4—Calibrated hot box test facility.

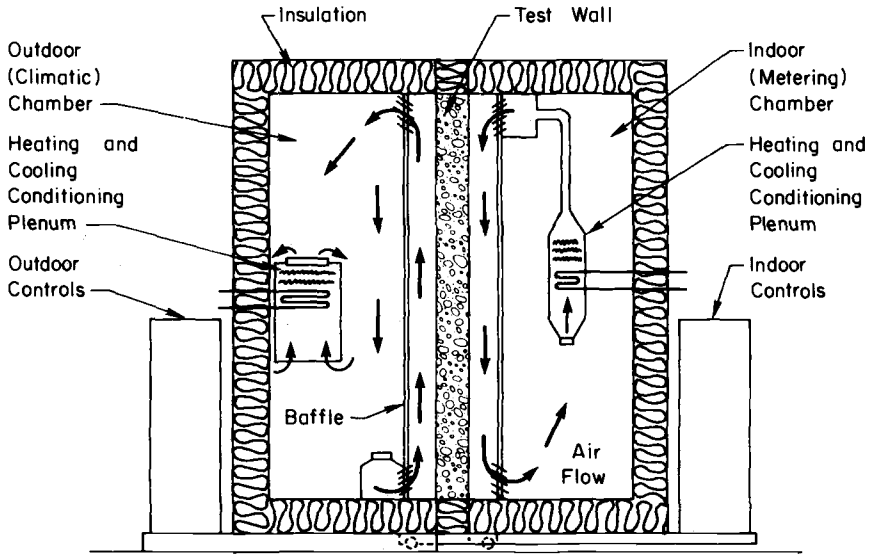


FIG. 5—Schematic of a calibrated hot box.

where

- $Q_w$  = heat transfer through the wall from the outdoor chamber to the indoor chamber,
- $Q_c$  = heat removed by indoor chamber cooling,
- $Q_h$  = heat supplied by indoor electrical resistance heaters,
- $Q_{fan}$  = heat supplied by the indoor circulation fan,
- $Q_f$  = heat gain (loss) from the laboratory, and
- $Q_j$  = heat gain (loss) to the indoor chamber from the flanking path around the specimen.

The units for the terms of Eq 1 are watt-hours per hour (British thermal units per hour).

A watt-hour transducer is used to measure  $Q_h$  and  $Q_{fan}$ . The value of  $Q_f$  is calculated from measured laboratory and indoor chamber temperatures. Heat flux transducers are used to check calculations of  $Q_f$ . Heat removed by indoor chamber cooling,  $Q_c$ , is calculated from the refrigerant enthalpy and mass flow rate, assuming an ideal basic vapor compression refrigeration cycle. Steady-state calibrated hot box tests of two "standard" calibration specimens were used to adjust for inefficiencies in the actual refrigeration cycle and to determine  $Q_f$ . In addition to flanking losses, other miscellaneous losses from the indoor chamber are included in  $Q_j$ .

### Steady-State Tests

Two steady-state calibrated hot box tests were performed on the walls with and without expanded perlite insulation. Energy and temperature measurements were used to calculate the average thermal properties, including total thermal resistance,  $R_T$ , and transmittance,  $U$ .

Design heat transmission coefficients were calculated for the walls and compared with measured values. The results were compared with values for NBS Test Building 6 walls.



### Measured Heat Transmission Coefficients

Steady-state calibrated hot box tests were conducted by maintaining constant indoor and outdoor chamber temperatures. Resistances were determined from data collected when specimen temperatures reached equilibrium and the rate of heat flow through the test wall was constant.

Total resistance values were calculated using measured values of heat flux and standard surface resistances equal to  $0.12 \text{ m}^2 \cdot \text{K}/\text{W}$  ( $0.68 \text{ h} \cdot \text{ft}^2 \cdot ^\circ\text{F}/\text{Btu}$ ) for the indoor surface and  $0.03 \text{ m}^2 \cdot \text{K}/\text{W}$  ( $0.17 \text{ h} \cdot \text{ft}^2 \cdot ^\circ\text{F}/\text{Btu}$ ) for the outdoor surface. These values are commonly used in design and are considered to represent still air on the indoor wall surface and an air flow of  $24 \text{ km}/\text{h}$  ( $15 \text{ mph}$ ) on the outdoor wall surface.

Steady-state tests were run at two temperature differentials. For the first case, indoor air temperature was maintained at approximately  $23^\circ\text{C}$  ( $73^\circ\text{F}$ ) while outdoor air temperature was maintained at approximately  $52^\circ\text{C}$  ( $125^\circ\text{F}$ ). This provided a nominal temperature differential of approximately  $29^\circ\text{C}$  ( $53^\circ\text{F}$ ) and a mean temperature of  $38^\circ\text{C}$  ( $100^\circ\text{F}$ ). Measured total resistances for Walls M9 and M10 under these conditions were  $0.59 \text{ m}^2 \cdot \text{K}/\text{W}$  ( $3.37 \text{ h} \cdot \text{ft}^2 \cdot ^\circ\text{F}/\text{Btu}$ ) and  $1.67 \text{ m}^2 \cdot \text{K}/\text{W}$  ( $9.47 \text{ h} \cdot \text{ft}^2 \cdot ^\circ\text{F}/\text{Btu}$ ), respectively.

In the second case, indoor air temperature was maintained at approximately  $21^\circ\text{C}$  ( $70^\circ\text{F}$ ) while outdoor air temperature was maintained at approximately  $-23^\circ\text{C}$  ( $-10^\circ\text{F}$ ). This provided a nominal temperature differential of  $44^\circ\text{C}$  ( $80^\circ\text{F}$ ) and a mean temperature of  $-1^\circ\text{C}$  ( $30^\circ\text{F}$ ). Measured total resistances for Walls M9 and M10 under these conditions were  $0.64 \text{ m}^2 \cdot \text{K}/\text{W}$  ( $3.64 \text{ h} \cdot \text{ft}^2 \cdot ^\circ\text{F}/\text{Btu}$ ) and  $1.64 \text{ m}^2 \cdot \text{K}/\text{W}$  ( $9.32 \text{ h} \cdot \text{ft}^2 \cdot ^\circ\text{F}/\text{Btu}$ ), respectively.

### Design Heat Transmission Coefficients

Design values of total resistance for Walls M9 and M10 and NBS Test Building 6 walls were calculated in accordance with procedures established by the American Society of Heating, Refrigerating, and Air-Conditioning Engineers [10]. Resistances for construction materials were taken from the *ASHRAE Handbook—1981 Fundamentals* [10] and the *Concrete Masonry Handbook* [11]. Standard surface resistances given in the Measured Heat Transmission Coefficients portion of this section were used.

The isothermal planes (series-parallel) method of calculating resistances was used to determine reduced wall resistances due to metal ties spanning the cavity. Reduced resistance due to insulation voids in the cavity of Wall M10 was also calculated using the isothermal planes method. As mentioned in the Test Specimens section, 3% of the cavity area perpendicular to heat flow was void of insulation.

Design values of total resistance for Wall M9, Wall M10, and NBS Test Building 6 walls were 0.61, 1.56, and  $2.37 \text{ m}^2 \cdot \text{K}/\text{W}$  (3.46, 8.83, and  $13.48 \text{ h} \cdot \text{ft}^2 \cdot ^\circ\text{F}/\text{Btu}$ ), respectively. Reference 7 describes design resistance calculations more thoroughly.

### Thermal Resistance Comparisons

The total thermal resistance values,  $R_T$ , for Walls M9 and M10 are summarized in Table 1. The design values are within 6% of the calibrated hot box test results for Walls M9 and M10. The total thermal resistance of the 300-mm (12-in.) cavity wall was increased 170% by the addition of perlite insulation.

Table 1 also lists thermal resistances of a wall similar to NBS Test Building 6 walls measured by Dynatech R/D Company [12]. The wall tested at Dynatech R/D was built by the same contractor who built the NBS test building. Tests were performed in accordance with the ASTM Test for Steady-State Thermal Performance of Building Assemblies by Means of a Guarded Hot Box (C 236-80). The design resistances calculated by Dynatech R/D Company [12] are also

TABLE 1—Total thermal resistance,  $R_T$ .

Wall Designation	Wall Description	Calculated (Design) $R_T$ , $m^2 \cdot K/W$ ( $h \cdot ft^2 \cdot ^\circ F/Btu$ )	Measured $R_T$ , $m^2 \cdot K/W$ ( $h \cdot ft^2 \cdot ^\circ F/Btu$ )	Mean Wall Temperature, $^\circ C$ ( $^\circ F$ )	Calculated $R_T$ /Measured $R_T$ Ratio
M9	300-mm (12-in.) block-brick cavity wall	0.61 <sup>a</sup> (3.46)	0.61 <sup>b</sup> (3.48)	22 (72)	0.99
M10	300-mm (12-in.) block-brick cavity wall with perlite	1.56 <sup>c</sup> (8.83)	1.66 <sup>b</sup> (9.41)	22 (72)	0.94
NBS	400-mm (16-in.) cavity wall with perlite; NBS Test Building 6 walls	2.69 <sup>d</sup> [12] (15.29)	2.21 <sup>e</sup> [12] (12.53)	2 to 3 (35 to 37)	1.22
		2.61 <sup>d</sup> [12] (14.83)	2.15 <sup>e</sup> [12] (12.19)	10 to 11 (50 to 53)	1.22
		2.37 <sup>a</sup> (13.48)	...	22 (72)	...

<sup>a</sup> Considering the effect of metal ties.

<sup>b</sup> Interpolated from calibrated hot box test results.

<sup>c</sup> Considering the effects of metal ties and expanded perlite settlement.

<sup>d</sup> Ignoring the effect of metal ties and expanded perlite settlement.

<sup>e</sup> Measured values were determined by Dynatech on a wall similar to those used in NBS Test Building 6.

The design values from Ref 12 of NBS Test Building 6 walls do not consider the effects of metal ties or insulation settlement. The calculated  $R_T$  values would be lower, and therefore closer to the measured values, if these effects were considered.

### Dynamic Tests

Exterior building walls are seldom in a steady-state condition. Outdoor air temperatures and solar effects cause cyclic changes in outdoor surface temperatures. Generally, indoor surface temperatures are relatively constant compared with outdoor surface temperatures.

Dynamic tests are a means of evaluating thermal response under controlled conditions that simulate temperature changes actually encountered in building envelopes. The response of walls to temperature changes is a function of both thermal resistance and heat storage capacity.

### Test Procedures

Since outdoor temperature conditions are frequently similar for several consecutive days, they may be assumed to follow a 24-h periodic cycle. Dynamic tests were conducted by maintaining a constant calibrated hot box indoor air temperature while outdoor air temperatures were cycled over a predetermined time-versus-temperature relationship. The rate of heat flow through a test specimen was determined from hourly averages of data.

One 24-h (diurnal) temperature cycle, denoted the NBS test cycle, has been applied to every wall tested in the calibrated hot box. This cycle is based on a simulated sol-air<sup>2</sup> cycle used by the National Bureau of Standards in their evaluation of dynamic thermal performance of an experimental masonry building [13]. It represents a large variation in outdoor temperature over a 24-h period. The mean outdoor temperature of the cycle is approximately equal to the mean indoor temperature.

Dynamic performance is dependent on the temperature cycle applied to the test specimen. Use of the NBS test cycle permits dynamic performance comparisons of all wall assemblies tested in the calibrated hot box [1-6].

Two additional sol-air diurnal temperature cycles were applied to the 300-mm (12-in.) cavity walls with and without expanded perlite fill. Outdoor surface temperatures of the west wall of NBS Test Building 6 were used to create cycles that produced similar outdoor surface temperatures on the test specimens. Dynamic test cycles, denoting the Gaithersburg April and Gaithersburg May cycles, respectively, were derived from data collected at the NBS test building from 10:00 A.M. 23 April 1982 through 10:00 A.M. 24 April 1982, and from 9:00 A.M. 31 May 1982 through 9:00 A.M. 1 June 1982. These 24-h cycles represent the third day of relatively repetitive daily temperature conditions at the NBS test site.

For all tests, the dynamic cycles were repeated until conditions of equilibrium were obtained. Equilibrium conditions were evaluated by consistency of applied temperatures and measured energy response. Each test required approximately six to eight days for completion. After equilibrium conditions were reached, the tests were generally continued for a period of three days. The results are based on average readings for at least three consecutive 24-h cycles, unless otherwise noted.

<sup>2</sup>Sol-air temperature is the temperature of outdoor air that, in the absence of all radiation exchanges, would give the same rate of heat entry into the surface as would exist with the actual combination of incident solar radiation, radiant energy exchange, and convective heat exchange with outdoor air [10].

## Dynamic Test Results

### Measured Temperatures and Heat Flux

Measured temperatures for dynamic temperature cycles applied to Walls M9 and M10 are illustrated in Figs. 6, 7, and 8. For Walls M9 and M10, the outdoor air,  $t_o$ , outdoor surface,  $t_2$ , indoor air,  $t_i$ , and indoor surface,  $t_1$ , temperatures are average readings of 16 thermocouples placed as described in the Test Specimens section of this paper. The internal block surface temperatures,  $t_3$ , and internal brick surface temperatures,  $t_4$  are average-readings of thermocouples placed on the block and brick surfaces, respectively, facing the cavity.

The measured and calculated heat flux values are illustrated in Figs. 9, 10, and 11. Heat flux determined from calibrated hot box tests is denoted  $q_w$ . Heat flux is positive when heat flows from the calibrated hot box outdoor chamber to the indoor chamber.

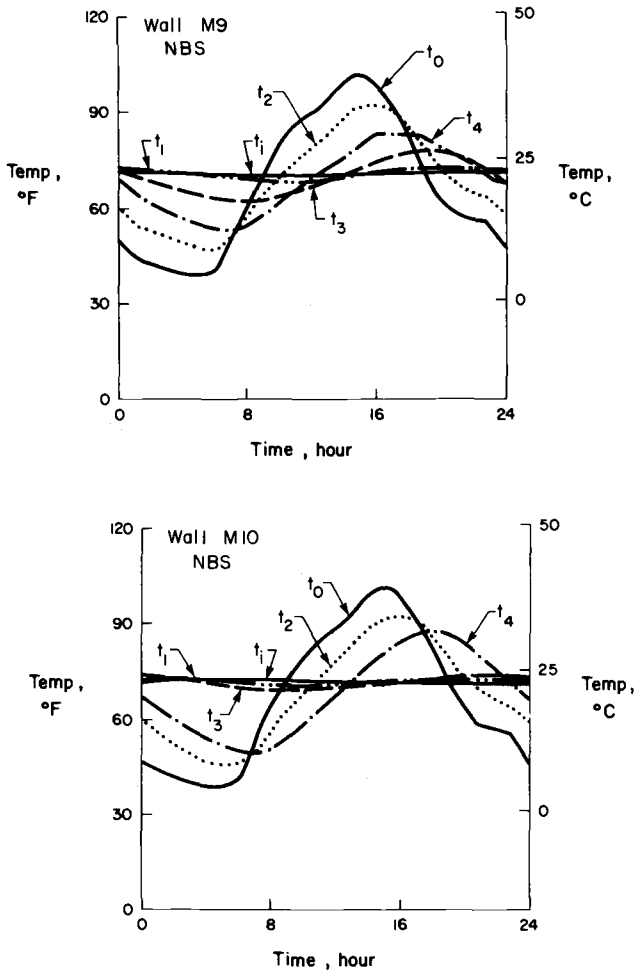


FIG. 6—Measured temperatures for the NBS test cycle: (top) Wall M9 (no insulation in the cavity); (bottom) Wall M10 (insulation in the cavity).

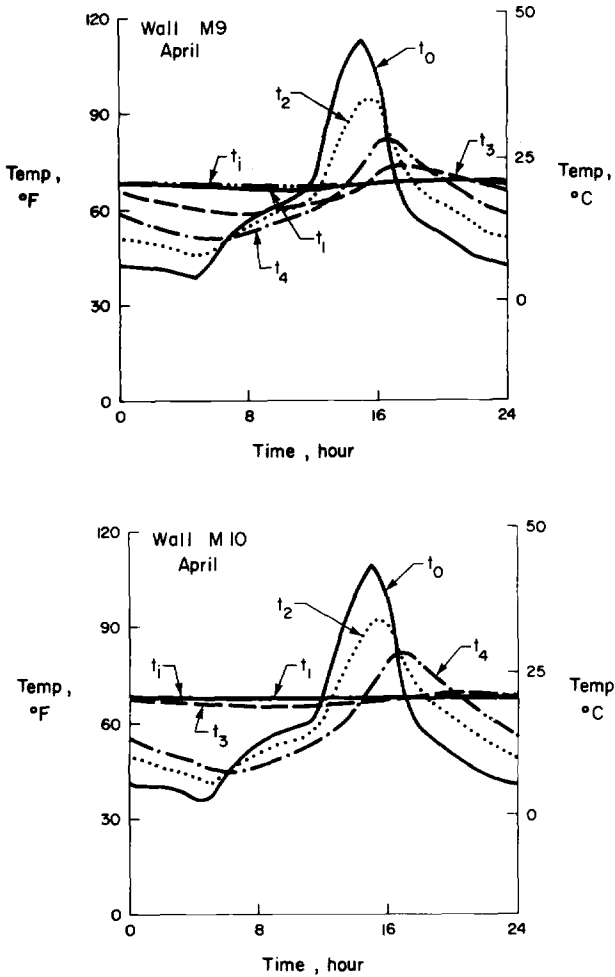


FIG. 7—Measured temperatures for the Gaithersburg April test cycle: (top) Wall M9 (no insulation in the cavity); (bottom) Wall M10 (insulation in the cavity).

Heat flux predicted by steady-state analysis is denoted  $q_{ss}$ . The values were calculated on an hourly basis from wall surface temperatures using the following equation

$$q_{ss} = \frac{(t_2 - t_1)}{R} \tag{2}$$

where

- $q_{ss}$  = heat flux through the wall predicted by steady-state analysis,  $W/m^2$  ( $Btu/h \cdot ft^2$ ),
- $R$  = average thermal resistance of the wall,  $m^2 \cdot K/W$  ( $h \cdot ft^2 \cdot ^\circ F/Btu$ ),
- $t_2$  = average temperature of the outdoor wall surface,  $^\circ C$  ( $^\circ F$ ), and
- $t_1$  = average temperature of the indoor wall surface,  $^\circ C$  ( $^\circ F$ ).

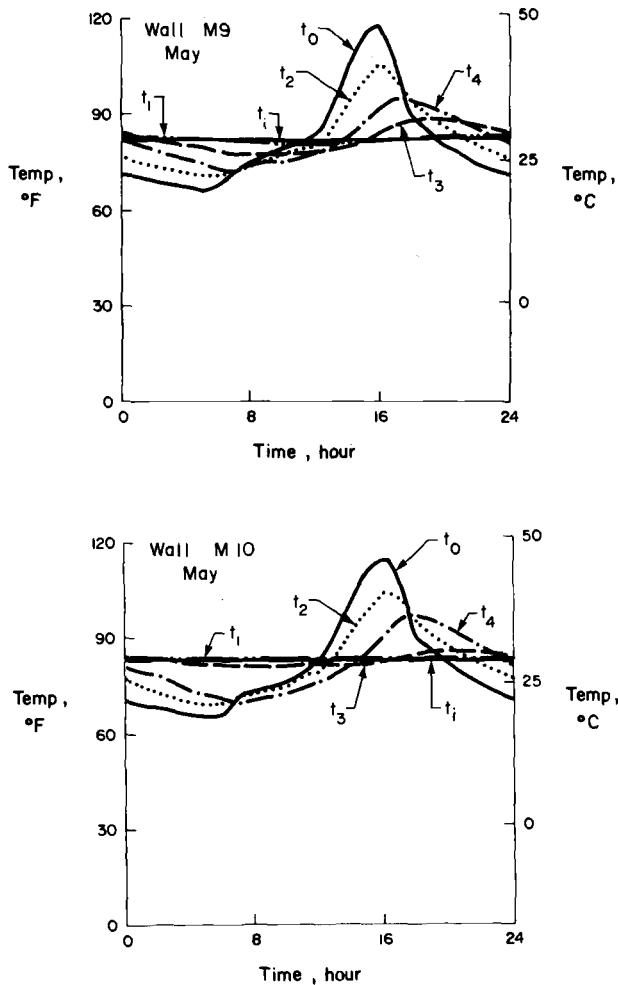


FIG. 8—Measured temperatures for the Gaithersburg May test cycle: (top) Wall M9 (no insulation in the cavity); (bottom) Wall M10 (insulation in the cavity).

Resistances for Walls M9 and M10 were derived from steady-state calibrated hot box tests. The resistance for the west wall of NBS Test Building 6 was determined from Dynatech R/D Company guarded hot box test results [12].

Descriptions of the symbols used in the figures appear in the Nomenclature section.

### Heat Flux Comparisons

Figures 9, 10, and 11 illustrate heat flux measured by the calibrated hot box,  $q_w$ , and calculated using steady-state theory,  $q_{ss}$ , for Walls M9 and M10. The measured heat flux is less than the calculated heat flux for both the wall without perlite insulation (Wall M9) and the wall with perlite insulation (Wall M10). Both the measured heat flux,  $q_w$ , and calculated heat flux,  $q_{ss}$ ,

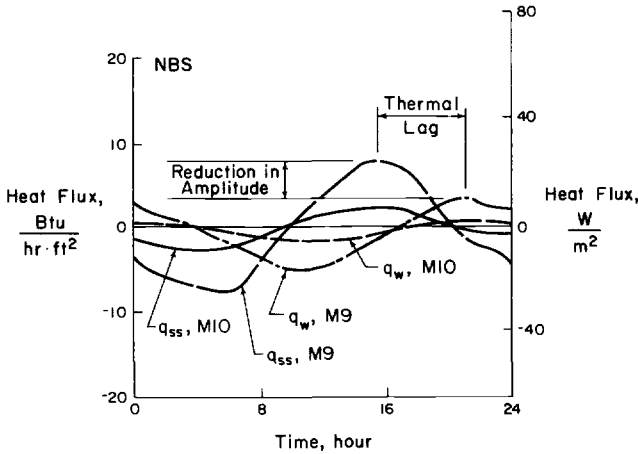


FIG. 9—Heat flux for the NBS cycle applied to Walls M9 and M10.

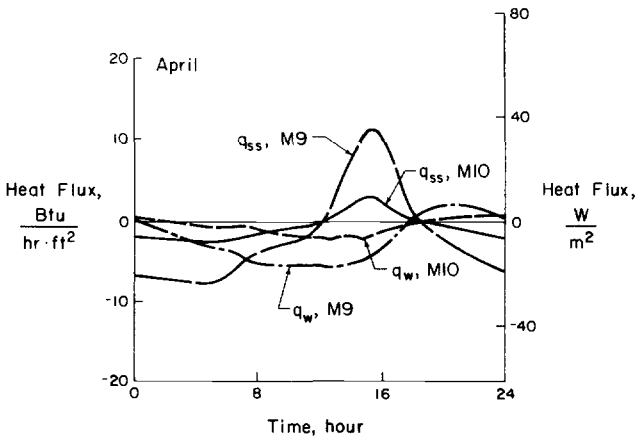


FIG. 10—Heat flux for the Gaithersburg April cycle applied to Walls M9 and M10.

are reduced for Wall M10 because of the addition of perlite insulation. The figures also show the shift in peaks, or thermal lag, from Wall M9 to Wall M10.

Figures 12 and 13 show calibrated hot box measurements for the Gaithersburg April and May test cycles, respectively, and measurements at NBS Test Building 6 for the same time period. The heat flux values measured by a heat flux transducer located on the west wall of NBS Test Building 6 are denoted  $q_{NBS}$  and were supplied by D. Burch of NBS.

For the Gaithersburg April test cycle (Fig. 12), calibrated hot box results for Wall M10 show less heat loss from the indoor environment than results from the NBS test building wall. The difference may be due to the test building wall having a cooler temperature history than the wall tested in the calibrated hot box (Wall M10).

Wall M10 was in the calibrated hot box approximately three days before dynamic equilib-

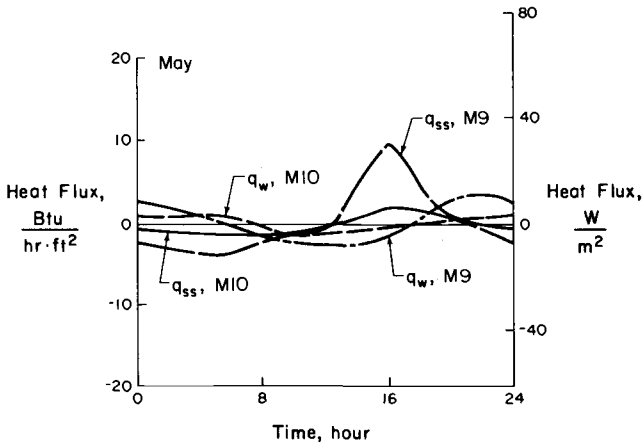


FIG. 11—Heat flux for the Gaithersburg May cycle applied to Walls M9 and M10.

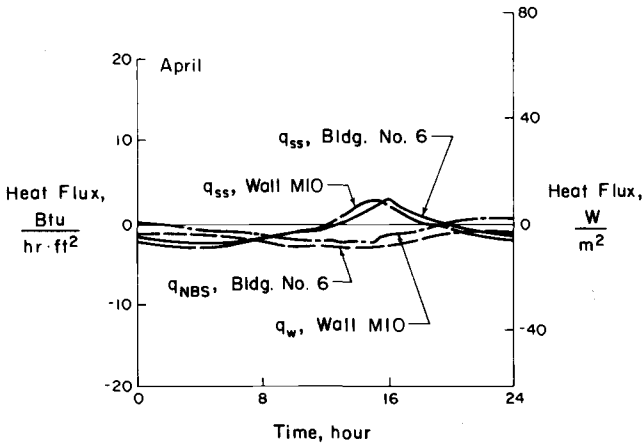


FIG. 12—Heat flux for Wall M10 and NBS Test Building 6 for the Gaithersburg April test cycle.

rium was reached. Dynamic equilibrium occurs when the measured temperatures and heat flux for the wall are relatively constant from day to day at any particular hour of the test cycle. The three-day temperature history for the NBS test building wall is shown in Fig. 14. The measured outdoor surface and indoor air temperatures are illustrated. Temperatures measured during dynamic equilibrium in the calibrated hot box are also shown in Fig. 14.

The average temperatures of the test building wall, on 22 and 23 April were 1.1°C (1.7°F) and 1.7°C (2.7°F) cooler, respectively, than those applied to Wall M10 during the Gaithersburg April test cycle. Temperatures for the third day preceding the comparative data may also have been cooler than temperatures for Wall M10. A cooler time history results in more heat loss from the indoor environment than predicted because temperatures within the wall are cooler than predicted.



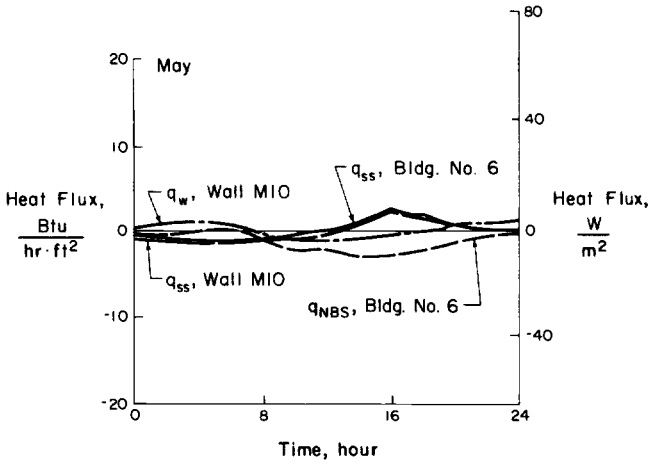


FIG. 13—Heat flux for Wall M10 and NBS Test Building 6 for the Gaithersburg May test cycle.

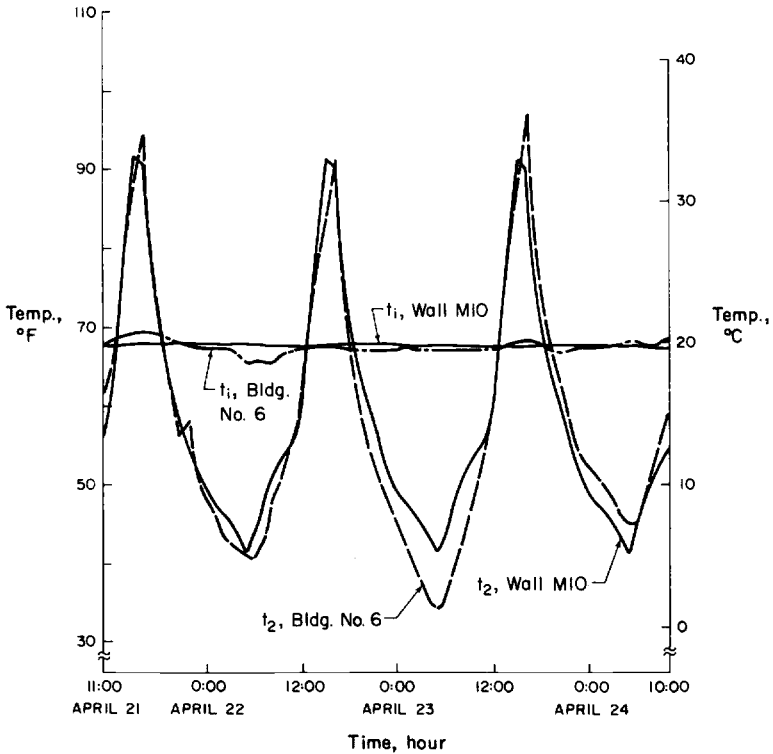


FIG. 14—April temperatures for NBS Test Building 6 and Wall M10.

Figure 13 shows that the measured heat loss for the Gaithersburg May cycle is also greater for the NBS test building wall than for Wall M10. The three-day temperature history for the NBS test building wall is shown in Fig. 15. Indoor air temperatures steadily rose during the three-day period; therefore, temperatures within the NBS test building wall might have been cooler than those within Wall M10.

Heat flux transducer measurements from the NBS test building wall may be lower than predicted for three reasons. First, the data comparisons were for sunny days during months when the average daily temperatures are generally increasing. Cooler temperatures within the wall cause more heat loss from the indoor environment than predicted. Heat energy is required to raise the average daily temperature of massive walls.

Second, the heat flux transducer readings were taken over a 50-mm (2-in.)-square area, and were instantaneous hourly readings. Therefore, the readings might not accurately reflect the integrated heat flux for the entire wall.

Third, the 400-mm (16-in.) wall was thick compared with the overall test building, which was 6.1 m (20 ft) square. Heat flow through the wall might have been two- or three-dimensional, rather than one-dimensional, as assumed. Heat distribution and transmission through the building slab and roof might have influenced heat flux through walls.

#### *Thermal Lag and Reduction in Amplitude*

Thermal lag and reduction in amplitude are used to describe wall dynamic thermal performance for a particular dynamic temperature cycle. Thermal lag, as illustrated in Fig. 9, is the difference in time between the actual heat flow,  $q_w$  or  $q_{NBS}$ , and the heat flow based on steady-state predictions,  $q_{ss}$ . Thermal lag is of interest because the time of occurrence of peak heat flows will have an effect on the overall response of the building envelope. If the envelope can be

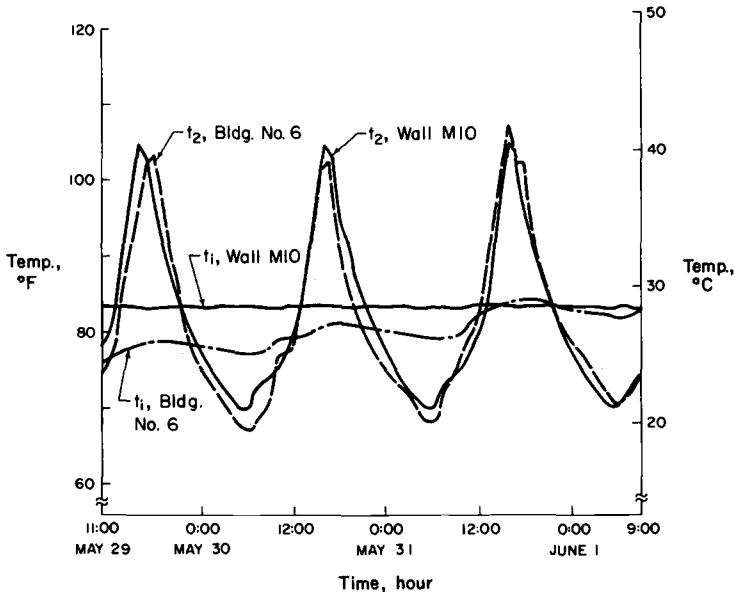


FIG. 15—May temperatures for NBS Test Building 6 and Wall M10.

used effectively to delay the occurrence of peak loads, it may be possible to improve overall energy efficiency. The "lag effect" is also of interest for passive solar applications.

The reduction in amplitude is the percentage reduction in actual peak heat flow compared with peak heat flow calculated using steady-state theory. The actual maximum heat flow through a wall is important in determining the peak energy load for a building envelope. Using actual peak heat flow rather than heat flow based on steady-state theory may reduce peak energy demands.

Thermal lag and reduction in amplitude are dependent on both the thermal resistance,  $R$ , and heat storage capacity

$$\rho cL$$

where

- $\rho$  = wall density,  $\text{kg/m}^3$  ( $\text{lb/ft}^3$ ),
- $c$  = wall specific heat,  $\text{J/kg} \cdot \text{K}$  ( $\text{Btu/lb} \cdot ^\circ\text{F}$ ), and
- $L$  = wall thickness,  $\text{m}$  ( $\text{ft}$ ).

Mass,  $\rho L$ , is the predominant factor in determining the heat storage capacity of most building materials.

For homogeneous walls, thermal lag and reduction in amplitude have been shown to increase with an increase in the dimensionless parameter,  $M$  [14]

$$M = \left( \frac{L^2/\alpha}{P} \right)^{1/2} = \left( \frac{(\rho cL) \cdot (R)}{P} \right)^{1/2} \quad (3)$$

where

- $L$  = wall thickness,  $\text{m}$  ( $\text{ft}$ ),
- $\alpha$  = thermal diffusivity,  $k/\rho c$ ,  $\text{m}^2/\text{s}$  ( $\text{ft}^2/\text{h}$ ),
- $k$  = thermal conductivity of wall,  $\text{W/m} \cdot \text{K}$  ( $\text{Btu/h} \cdot \text{ft} \cdot ^\circ\text{F}$ ),
- $\rho$  = wall density,  $\text{kg/m}^3$  ( $\text{lb/ft}^3$ ),
- $c$  = wall specific heat,  $\text{J/kg} \cdot \text{K}$  ( $\text{Btu/lb} \cdot ^\circ\text{F}$ ),
- $R$  = wall resistance,  $\text{m}^2 \cdot \text{K/W}$  ( $\text{h} \cdot \text{ft}^2 \cdot ^\circ\text{F/Btu}$ ), and
- $P$  = period of dynamic cycle,  $\text{h}$ .

The parameter  $M$  is equal to the square root of the ratio of two measurements of time. The numerator,  $L^2/\alpha$ , is a measurement of time required for the wall to thermally respond to a change in temperature. The denominator,  $P$ , is the time required to complete a cycle. Dynamic temperature cycles generally can be assumed to have a period,  $P$ , of 24 h.

Changes in  $R$  affect the dynamic parameters of thermal lag and reduction in amplitude, as well as alter the maximum heat flux predicted by steady-state analysis. Changes in heat storage capacity affect only the dynamic parameters of thermal lag and reduction in amplitude.

The principles discussed in the last two paragraphs are valid for multilayered wall assemblies even though Eq 3 is derived for homogeneous walls only. Childs [14] suggests using the sum of  $M$  values for each wall layer as an approximate method of predicting lag and reduction in amplitude.

Table 2 lists material properties used to calculate  $M'$  values for individual layers of Wall M9, Wall M10, and NBS Test Building 6 walls.

$$M' = (L^2/\alpha)^{1/2} = (\rho cL \cdot R)^{1/2} \quad (4)$$

TABLE 2—Calculation of M' values for individual wall layers.

Wall Designation	Wall Layer	R, Thermal Resistance, $m^2 \cdot K/W$ ( $h \cdot ft^2 \cdot ^\circ F/Btu$ )	$\rho$ , Unit Weight, $kg/m^3$ ( $lb/ft^3$ )	$c_p$ , Specific Heat, $J/kg \cdot K$ ( $Btu/lb \cdot ^\circ F$ )	$L^b$ , Equivalent Thickness, $m$ (ft)	$\rho c L$ , Storage Capacity, $W \cdot h/K \cdot m^2$ ( $Btu/^\circ F \cdot ft^2$ )	$M'$ , $(\rho c L \cdot R)^{1/2}$ , $(h)^{1/2}$
M9	brick	0.08 (0.44)	2160 <sup>c</sup> (135)	800 (0.19)	0.070 (0.23)	33.5 (5.90)	1.61
	air	0.17 (0.97)	0	...	...	0	0
	block	0.21 (1.18)	2000 <sup>c</sup> (125)	840 (0.20)	0.079 (0.26)	36.9 (6.50)	2.77
	plaster	0.01 (0.03)	1860 (116)	840 (0.20)	0.003 (0.01)	1.3 (0.24)	0.08
M10	brick	0.08 (0.44)	2160 <sup>c</sup> (135)	800 (0.19)	0.070 (0.23)	33.5 (5.90)	1.61
	perlite	1.51 (8.59)	69 (4.3)	1090 (0.26)	0.070 (0.23)	1.5 (0.26)	1.49
	block	0.21 (1.18)	2000 <sup>c</sup> (125)	840 (0.20)	0.079 (0.26)	36.9 (6.50)	2.77
	plaster	0.01 (0.03)	1860 (116)	840 (0.20)	0.003 (0.01)	1.3 (0.24)	0.08
NBS	brick	0.08 (0.44)	2160 (135)	800 (0.19)	0.070 (0.23)	33.5 (5.90)	1.61
	perlite	1.93 (10.94)	69 (4.3)	1090 (0.26)	0.089 (0.29)	1.82 (0.32)	1.87
	block	0.30 (1.68)	1680 (105)	840 (0.20)	0.11 (0.35)	41.7 (7.35)	3.51
	plaster	0.02 (0.10)	1860 (116)	840 (0.20)	0.012 (0.04)	5.31 (0.93)	0.31

<sup>a</sup> Values of specific heat are determined from Refs 10 and 15.  
<sup>b</sup> Equivalent thicknesses for block and brick are equal to the product of the layer width and percentage of solid volume.  
<sup>c</sup> Unit weight is equal to the sum of the oven-dry unit weight of the material and estimated moisture content.

The term  $P$  is omitted from the equation for  $M'$  because all walls are tested using cycles with a constant  $P$ , equal to 24 h. The thermal resistances are from Refs 10 and 11 and do not include surface resistances. Unit weights of block and brick for Walls M9 and M10 are determined from measured oven-dry material unit weights and estimated moisture contents. The unit weight of perlite used in Wall M10 is measured. Other unit weights are estimated using properties listed in Ref 10. Values of specific heat are determined from Refs 10 and 15. The equivalent thicknesses for block and brick are equal to the product of the layer width and percentage of solid volume.

The last two columns of Table 2 list heat storage capacity,  $\rho cL$ , and  $M'$  values,  $(\rho cL \cdot R)^{1/2}$ , for each layer of the walls. The expanded perlite layers have  $M'$  values within the same range as the brick and block layers. Expanded perlite has relatively high thermal resistance and low storage capacity, while brick and block have low resistances and high storage capacities.

Table 3 lists  $M'$  values, thermal lag, and percentage of reduction in amplitude for Wall M9, Wall M10, and NBS Test Building 6 walls, denoted NBS. Values of  $M'$  for individual wall layers are summed to determine total wall  $M'$  values. The thermal lag and percentage of reduction in amplitude for Walls M9 and M10 are measured using the calibrated hot box. The values for NBS Test Building 6 are measured field data from a heat flux transducer mounted on the west wall.

Table 3 shows that measured thermal lag and calculated  $M'$  increase with the addition of expanded perlite insulation to the 300-mm (12-in.) cavity wall. The addition of expanded perlite insulation increases  $M'$  from 4.5, for Wall M9, to 6.0 (h)<sup>1/2</sup>, for Wall M10.

Table 3 also shows that thermal lags increase with an increase in  $M'$  for walls with insulation, Walls M10 and NBS. The 400-mm (16-in.) insulated cavity wall, denoted NBS, has greater thermal lags and  $M'$  than the 300-mm (12-in.) insulated cavity wall, denoted M10.

Reduction in amplitude remains relatively constant when expanded perlite insulation is added to the 300-mm (12-in.) cavity wall. Table 3 shows that reduction in amplitude values range from 43 to 51% for all cycles on Walls M9 and M10.

The thermal lags and reductions in amplitude for the April and May data from the NBS test building wall differ more than those determined from calibrated hot box tests. The differences may be due to variability in heat flux transducer data or any of the phenomena described in the Heat Flux Comparisons portion of this section.

**Total Energy Requirements**

The results of dynamic tests for Walls M9 and M10 were also compared using measurements of energy expended in maintaining constant indoor temperature while outdoor temperatures were varied. The energy expended is a measurement of heat flow through the test wall.

TABLE 3—Dynamic parameters of walls.

Wall Designation	Calculated $M'$ , h <sup>1/2</sup>	Wall Properties					
		Measured Thermal Lag, h, for Test Cycle			Measured Reduction in Amplitude, %, for Test Cycle		
		NBS	April	May	NBS	April	May
M9	4.46	5.5	5	6.5	43	51	49
M10	5.95	7	7.5	7.5	50	44.5	47
NBS	7.30	8.4	8.4	12	...	51	5

The measured and calculated total energy requirements for the NBS Gaithersburg April and Gaithersburg May test cycles applied to Walls M9 and M10 are summarized in Table 4. The curves marked  $q_w$  in Figs. 9 through 13 are measurements of heat flow through the test wall. The sum of the areas between each  $q_w$  curve and the zero heat flow rate line is taken to represent the total energy over a 24-h period. This value is denoted  $q_w^T$  in Table 4. A similar procedure is used to calculate the total energy over a 24-h period for predictions based on steady-state analysis. These values are denoted  $q_{ss}^T$  in Table 4.

The addition of expanded perlite fill to the masonry cavity of Wall M9 to form Wall M10 reduces the total energy requirements by 66 to 68%, as shown in the columns labeled Measured Total Energy Comparisons and Calculated Total Energy Comparisons. The results are consistent for both measured and calculated values. This reduction in energy requirements is due to the increased thermal resistance of the expanded perlite-filled walls.

Table 4 also shows that the measured total energy,  $q_w^T$ , for each cycle, is less than the total energy predicted by steady-state analysis,  $q_{ss}^T$ . The measured total energy ranges from 57 to 62% of the calculated total energy for all three test cycles on both walls. This is due to the wall storage capacity and reversals of heat flow through each wall. When the NBS Gaithersburg April and Gaithersburg May test cycle are applied to walls during the calibrated hot box tests, the outdoor wall surface temperatures fluctuate above and below the indoor wall surface temperatures, which causes reversals of heat flow through the walls. For example, during the NBS test cycle, the outdoor surface temperatures vary from approximately 10 to 38°C (50 to 100°F) while indoor surface temperatures vary in the range of 21 to 24°C (70 to 75°F).

For walls subjected to reversals in heat flow, total heat flow entering and leaving the indoor surface is reduced compared to steady-state predictions. The amount of heat flow entering or leaving the indoor surface is not as great as that predicted by steady-state analysis because steady-state equilibrium is never achieved within the wall. Heat storage within the wall reduces temperature fluctuations on the indoor surface.

It should be noted that comparison of the measured energy values for test walls is limited to specimens and dynamic cycles evaluated in this program. The results are for diurnal test cycles and should not be arbitrarily assumed to represent annual heating and cooling loads. In addition, the results are for individual opaque wall assemblies; as such, they are representative of only one component of the building envelope.

## Summary and Conclusions

This report presents results of an experimental investigation of heat transmission characteristics for two block-brick cavity walls. Wall M9 contained no insulation. Wall M10 contained expanded perlite loose-fill insulation in the cavity. Tests were conducted under steady-state and dynamic temperature conditions. The results are compared with measured values from a test building with cavity walls monitored by the National Bureau of Standards in Gaithersburg, Maryland.

The following conclusions are based on results obtained in this investigation:

1. Measured overall thermal resistances,  $R_T$ , for Walls M9 and M10, respectively, were 0.61 and 1.66 m<sup>2</sup> · K/W (3.48 and 9.41 h · ft<sup>2</sup> · °F/Btu).
2. Design overall thermal resistances,  $R_T$ , for Walls M9 and M10 were within 6% of calibrated hot box test results.
3. Calibrated hot box results for the Gaithersburg April and Gaithersburg May test cycles on the wall with expanded perlite insulation (Wall M10), showed less heat loss from the indoor environment than heat flux transducer measurements from NBS Test Building 6.

TABLE 4—Measured and calculated total energy requirements.

Test Cycle	Measured Total Energy, $q_w^T$ , $W \cdot h/m^2$ (Btu/ft <sup>2</sup> )		Measured Total Energy Comparisons, With Perlite/Without Perlite Ratio		Calculated Total Energy, $q_{ts}^T$ , $W \cdot h/m^2$ (Btu/ft <sup>2</sup> )		Calculated Total Energy Comparisons, With Perlite/Without Perlite Ratio		Total Energy Comparisons, $\frac{q_w^T}{q_{ts}^T}$	
	Wall M9, Without Perlite	Wall M10, With Perlite	Wall M9, Without Perlite	Wall M10, With Perlite	Wall M9, Without Perlite	Wall M10, With Perlite	Wall M9, Without Perlite	Wall M10, With Perlite	Wall M9	Wall M10
NBS	219.1 (69.5)	70.0 (22.2)			382.4 (121.2)	122.8 (38.9)	0.32	0.32	0.57	0.57
Gaithersburg April	247.4 (78.4)	83.5 (26.5)			396.9 (125.8)	136.4 (43.2)	0.34	0.34	0.62	0.61
Gaithersburg May	151.5 (48.0)	50.2 (15.9)			243.3 (77.1)	80.7 (25.6)	0.33	0.33	0.62	0.62

delayed heat flow through the specimens. The thermal lag values range from 5 to 6.5 h for Wall M9, from 7 to 7.5 h for Wall M10, and from 8 to 12 h for the west wall of NBS Test Building 6.

5. Measured thermal lag increases for each dynamic cycle when expanded perlite is added to the cavity.

6. As indicated by the damping effect, the heat storage capacities of Walls M9 and M10 reduced peak heat flows through the specimens. Reduction in the amplitude values ranges from 43 to 51% for Wall M9 and from 45 to 50% for Wall M10.

7. For the three diurnal temperature cycles applied to Walls M9 and M10, energy requirements for a 24-h period were less than would be predicted by steady-state analysis. Total measured heat flows for the 24-h cycles ranged from 57 to 62% of those predicted by steady-state analysis, for both test specimens. These reductions in total heat flow are attributed to wall storage capacity and reversals in heat flow.

8. The addition of expanded perlite fill to the cavity wall reduces total heat flow by 66 to 68% for the three diurnal cycles. This reduction is due to the increased thermal resistance of the expanded-perlite-filled wall.

Results described in this paper provide data on the thermal response of masonry cavity walls subjected to steady-state and diurnal sol-air temperature cycles. A complete analysis of building energy requirements must include consideration of the entire building envelope, building orientation, building operation, and yearly weather conditions. Data developed in this experimental program provide a quantitative basis for modeling the building envelope, which is part of the overall energy analysis process.

### *Acknowledgments*

This paper was prepared as part of a project sponsored jointly by the Portland Cement Association, the Brick Institute of America, the National Concrete Masonry Association, and the Perlite Institute, Inc. The work was performed in the Engineering and Resource Development Division of the Construction Technology Laboratories (CTL), a Division of the Portland Cement Association, under the direction of Dr. W. G. Corley, executive director, and D. W. Musser, formerly director of the Construction Methods Department.

The brick for the cavity wall construction was provided by the Brick Institute of America. Silbrico Corp. supplied expanded perlite loose-fill insulation for the cavity. Metal ties were provided by Dur-o-Wall, Inc.

Data from NBS Test Building 6 for comparison with calibrated hot box test results were supplied by D. Burch, National Bureau of Standards. Information on NBS Test Building 6 wall construction was provided by A. Desjarlais, Dynatech R/D Company. S. C. Larson, associate research engineer, Fire Research Section, assisted with data reduction, reviewed the manuscript, and provided helpful comments and suggestions.

### **References**

- [1] Fiorato, A. E. and Cruz, C. R., "Thermal Performance of Masonry Walls," Research and Development Bulletin RD071, Portland Cement Association, Skokie, IL, 1980.
- [2] Fiorato, A. E., "Heat Transfer Characteristics of Walls Under Dynamic Temperature Conditions," Research and Development Bulletin RD075, Portland Cement Association, Skokie, IL, 1981.
- [3] Fiorato, A. E. and Bravinsky, E., "Heat Transfer Characteristics of Walls Under Arizona Temperature Conditions," Construction Technology Laboratories, Portland Cement Association, Skokie, IL, 1981.
- [4] Van Geem, M. G., Fiorato, A. E., and Julien, J. T., "Heat Transfer Characteristics of a Normal Weight Concrete Wall," Construction Technology Laboratories, Portland Cement Association, Skokie, IL, 1983.



- Concrete Wall," Construction Technology Laboratories, Portland Cement Association, Skokie, IL, 1983.
- [6] Van Geem, M. G. and Fiorato, A. E., "Heat Transfer Characteristics of a Low Density Concrete Wall," Construction Technology Laboratories, Portland Cement Association, Skokie, IL, 1983.
- [7] Van Geem, M. G. and Larson, S. C., "Heat Transfer Characteristics of a Masonry Cavity Wall With and Without Expanded Perlite Insulation," Construction Technology Laboratories, Portland Cement Association, Skokie, IL, 1984.
- [8] Burch, D. M., Remmert, W. E., Krintz, D. F., and Barnes, C. S., "A Field Study of the Effect of Wall Mass on the Heating and Cooling Loads of Residential Buildings," *Proceedings*, Thermal Mass Effects in Buildings Seminar, Knoxville, TN, June 1982, Oak Ridge National Laboratory, Oak Ridge, TN, 1983, pp. 265-312.
- [9] Fiorato, A. E., "Laboratory Tests of Thermal Performance of Exterior Walls," *Proceedings*, ASHRAE SP28, American Society of Heating, Refrigerating, and Air Conditioning Engineers/Department of Energy-Oak Ridge National Laboratory Conference on Thermal Performance of the Exterior Envelopes of Buildings, Orlando, FL, Dec. 1979, Atlanta, GA, 1981, pp. 221-236.
- [10] *ASHRAE Handbook—1981 Fundamentals*, American Society of Heating, Refrigerating, and Air Conditioning Engineers, Atlanta, GA, 1981.
- [11] Randall, F. A., Jr. and Panarese, W. C., *Concrete Masonry Handbook*, Bulletin EB008.04M, Portland Cement Association, Skokie, IL, 1980.
- [12] Desjarlais, A., "Thermal Conductance and Thermal Transmittance of Six Residential Wall Structures," Report No. NBS-3, Dynatech R/D Company, Cambridge, MA, 1982.
- [13] Peavy, B. A., Powell, F. J., and Burch, D. M., "Dynamic Thermal Performance of an Experimental Masonry Building," Building Science Series 45, U.S. Department of Commerce, National Bureau of Standards, Washington, DC, 1973.
- [14] Childs, K. W., Courville, G. E., and Bales, E. L., "Thermal Mass Assessment," Oak Ridge National Laboratory for the U.S. Department of Energy, Oak Ridge, TN, 1983.
- [15] Van Geem, M. G. and Fiorato, A. E., "Thermal Properties of Masonry Materials for Passive Solar Design—A State-of-the-Art Review," Construction Technology Laboratories, Portland Cement Association, Skokie, IL, 1983.